Semimicroscopic description of odd At isotopes*

V. Paar
Institute Rudjer Bošković, Zagreb, Yugoslavia
(Received 8 July 1974)

The properties of odd At isotopes have been described by coupling three valence-shell protons to the quadrupole vibrational field. Qualitative and quantitative results have been compared with recent experimental data from the Dubna and Stockholm groups. It is interesting to note that two lowest $7/2^-$ states exchange their character in At nuclei away from the $N = 126$ shell closure. This pronounced feature of At isotopes is a combined effect of the particle-vibration coupling and the Pauli principle.

[NUCLEAR STRUCTURE $^{203-211}$At; calculated spectra, electromagnetic properties. Three valence-shell particles coupled to quadrupole vibration.]

I. INTRODUCTION

The properties of ^{211}At have been extensively studied, both experimentally and theoretically. Experimental investigations have been performed by the radioactive decay of ^{211}Rn and by $(\alpha, 2n\gamma)$ "in-beam" spectroscopy.[1-7] Rather limited experimental information on $^{203, 205, 207, 209, 215, 217}$At has been obtained by studying the radioactive decay of the corresponding Rn isotopes.[8-14] Low-lying negative-parity states of ^{211}At have been calculated in the framework of restricted shell-model calculations involving the three protons outside the doubly magic ^{208}Pb nucleus. Shell-model calculations have been performed using the surface-δ interaction,[15] Wigner singlet and tensor force,[16-18] semirealistic matrix elements,[19] and empirical matrix elements from ^{210}Po.[20, 21] In Ref. 16 the coupling in lowest order to the 2^+ core state was included into the effective charge. In Ref. 22 the shell-model calculations with empirical matrix elements was performed only for $(h_{9/2}{}^3)$ configurations, including also the coupling to zero and one-quadrupole-phonon core excitations. No calculations for $^{203, 205, 207, 209, 215, 217}$At are available.

In the present paper we describe odd At isotopes by coupling three valence-shell protons to the quadrupole vibrational field (Alaga model).[23, 24] In this way important shell-model and collective features of these nuclei are accounted for.[24-27] The coexistence of both aspects seems to dominate in creating nuclear properties of At nuclei away from the $N=126$ closed shell (^{211}At).

II. CALCULATION

The Hamiltonian of the three-particle shell-model cluster–vibrational-field coupled system[24, 25, 28] is

$$H = H_{SH}^{(3)} + H_{\mathrm{VIB}} + H_{\mathrm{RES}} + k \sum_{i=1}^{3} \sum_{\mu=1}^{5} \alpha_2^{\mu} Y_2^{\mu *}(\theta_i, \phi_i) .$$

Here $H_{SH}^{(3)}$ describes the motion of three valence-shell particles (cluster), H_{VIB} represents the free quadrupole vibrational field, and H_{RES} is the residual interaction between the valence-shell particles. The last term represents the cluster-vibration interaction.

In the present calculation we use the proton single-particle energies from ^{209}Bi

$$\epsilon(f_{7/2}) - \epsilon(h_{9/2}) = 0.89 \text{ MeV},$$
$$\epsilon(f_{5/2}) - \epsilon(h_{9/2}) = 2.81 \text{ MeV},$$
$$\epsilon(i_{13/2}) - \epsilon(h_{9/2}) = 1.60 \text{ MeV}.$$

The bare phonon energy corresponds to the energy of the 2_1^+ state in the corresponding Pb vibrator nucleus. For ^{211}At the phonon energy $\hbar\omega_2(^{208}\mathrm{Pb}) = 4.07$ MeV, while for the other At isotopes the phonon energies from the corresponding Pb isotopes with open neutron shells are approximately 1 MeV. The bare particle-field coupling strength is roughly estimated as $a = (4\pi)^{1/2}/(3ZeR^2)\langle k\rangle \times [B^{\mathrm{VIB}}(E2)(2_1^+ \rightarrow 0_1^+)]^{1/2}$. Here $B^{\mathrm{VIB}}(E2)$ corresponds to vibrator nuclei and $\langle k\rangle \approx 50$ MeV.[28] For ^{207}At the bare coupling strength a is approximately 0.3. However, the Q-Q component of the bare residual force as well as high-frequency quadrupole modes and the isovector potential renormalize the bare particle-field coupling strength.[28, 29] In the present calculations only the pairing force was explicitly included in the residual interaction H_{RES}.[24, 25] The Hamiltonian is diagonalized in the basis built from three antisymmetrized shell-model particles of angular momentum J, coupled with an N-phonon state of angular momentum R

to the total angular momentum I. States up to two phonons have been included in the calculation. Figure 1 shows the calculated negative-parity spectra for parametrizations (I) $a=1$, (II) $a=0.5$, (III) $a=0.4$, (IV) $a=0.4$, and (V) $a=0.8$. In parametrizations I, II, and III we used a phonon energy $\hbar\omega_2$ of 1 MeV, and in parametrizations IV and V we employed a phonon energy $\hbar\omega_2$ of 4.07 MeV. In parametrizations I–V the pairing strength G was 0.15. In parametrization VI we used a particle-field coupling strength of 0.4, a pairing strength of 0.10, and a phonon energy of 0.84 MeV. Figure 2 shows the calculated positive-parity spectra for parametrizations III and V. Figure 3 represents the available experimental spectra. Table I lists the largest components of wave functions in parametrizations IV and III for ^{211}At and ^{205,207,209}At nuclei. Like ^{201,203,205}Tl isotopes, which have the same corresponding basic vibrators, ^{205,207,209}At nuclei also exhibit remarkable mutual similarity. Because of that and since we are not looking at details, the energies and wave functions in case III correspond approximately to ^{205,207,209}At nuclei.

The $E2$ and $M1$ operators in the cluster-vibration coupling model consist of a cluster and a vibrational part

$$M^{\mu}(E2)=\sum_{i=1}^{3} e^{\text{s.p.}} r_i^{\,2} Y_2^{\mu}(\theta_i,\phi_i)+\frac{3}{4\pi} e^{\text{VIB}} R_0^{\,2} \times[b_2^{\mu\dagger}+(-)^{\mu} b_2^{-\mu}],$$

$$\vec{\mathrm{M}}(M1)=\left(\frac{3}{4\pi}\right)^{1/2}[g_R\vec{\mathrm{I}}+(g_l-g_R)\vec{\mathrm{J}}+(g_s-g_l)\vec{\mathrm{S}}].$$

Here $e^{\text{s.p.}}$ and e^{VIB} are the single-particle and vibrator charge, respectively, and g_R, g_l, and g_s are the gyromagnetic ratios. The bare value

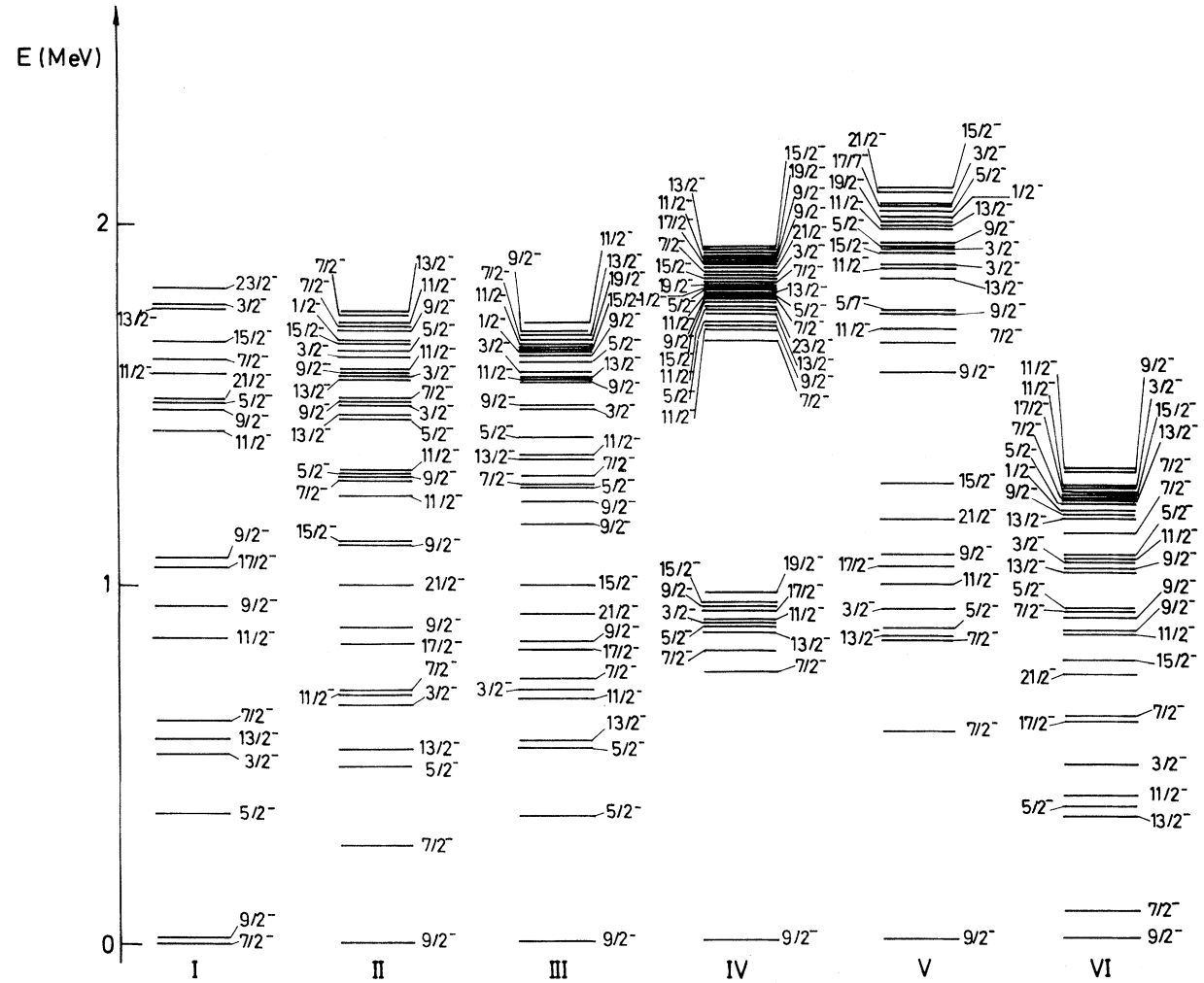

FIG. 1. Calculated negative-parity spectra of odd At isotopes. For description see Sec. II.

TABLE I. Largest components (≥9%) in the wave functions of negative-parity states of ^{205,207,209}At and ^{211}At and the shell-model wave functions of ^{211}At.

		^{205,207,209}At	^{211}At	
		Present	Present	Shell Model [a]
$\frac{9}{2}^-_1$	$\vert (h_{9/2}^3)\frac{9}{2}, 00; \frac{9}{2}\rangle$	0.83	0.93	0.95
$\frac{7}{2}^-_1$	$\vert (h_{9/2}^3)\frac{7}{2}, 00; \frac{7}{2}\rangle$	0.66	0.53	0.43
	$\vert (h_{9/2}^3)\frac{7}{2}, 12; \frac{7}{2}\rangle$	−0.33		
	$\vert (h_{9/2}^3)\frac{9}{2}, 12; \frac{7}{2}\rangle$	0.48		
	$\Vert (h_{9/2}^2)0, f_{7/2} \vert \frac{7}{2}, 00; \frac{7}{2}\rangle$		−0.78	−0.84
$\frac{7}{2}^-_2$	$\vert (h_{9/2}^3)\frac{7}{2}, 00; \frac{7}{2}\rangle$		0.81	0.90
	$\Vert (h_{9/2}^2)0, f_{7/2} \vert \frac{7}{2}, 00; \frac{7}{2}\rangle$	0.72	0.52	0.41
	$\Vert (h_{9/2}^2)0, f_{7/2} \vert \frac{7}{2}, 12; \frac{7}{2}\rangle$	−0.36		
$\frac{5}{2}^-_1$	$\vert (h_{9/2}^3)\frac{5}{2}, 00; \frac{5}{2}\rangle$	0.64	0.97	1.00
	$\vert (h_{9/2}^3)\frac{9}{2}, 12; \frac{5}{2}\rangle$	−0.58		
$\frac{13}{2}^-_1$	$\vert (h_{9/2}^3)\frac{13}{2}, 00; \frac{13}{2}\rangle$	0.71	0.97	1.00
	$\vert (h_{9/2}^3)\frac{9}{2}, 12; \frac{13}{2}\rangle$	−0.50		
$\frac{3}{2}^-_1$	$\vert (h_{9/2}^3)\frac{3}{2}, 00; \frac{3}{2}\rangle$	0.77	0.98	1.00
	$\vert (h_{9/2}^3)\frac{5}{2}, 12; \frac{3}{2}\rangle$	0.44		
$\frac{11}{2}^-_1$	$\vert (h_{9/2}^3)\frac{11}{2}, 00; \frac{11}{2}\rangle$	0.73	0.98	1.00
	$\vert (h_{9/2}^3)\frac{9}{2}, 12; \frac{11}{2}\rangle$	0.46		
$\frac{15}{2}^-_1$	$\vert (h_{9/2}^3)\frac{15}{2}, 00; \frac{15}{2}\rangle$	0.88	0.99	0.99
$\frac{17}{2}^-_1$				
	$\vert (h_{9/2}^3)\frac{17}{2}, 00; \frac{17}{2}\rangle$	0.82	0.98	0.99
	$\vert (h_{9/2}^3)\frac{13}{2}, 12; \frac{17}{2}\rangle$	−0.33		
$\frac{21}{2}^-_1$	$\vert (h_{9/2}^3)\frac{21}{2}, 00; \frac{21}{2}\rangle$	0.87	0.98	0.99
	$\vert (h_{9/2}^3)\frac{21}{2}, 12; \frac{21}{2}\rangle$	−0.33		
$\frac{3}{2}^-_2$	$\vert (h_{9/2}^3)\frac{7}{2}, 12; \frac{3}{2}\rangle$	0.36		
	$\Vert (h_{9/2}^2)2, f_{7/2} \vert \frac{3}{2}, 00; \frac{3}{2}\rangle$	−0.57	0.88	0.98
	$\Vert (h_{9/2}^2)0, f_{7/2} \vert \frac{7}{2}, 12; \frac{3}{2}\rangle$	0.50		
	$\Vert (h_{9/2}^2)4, f_{7/2} \vert \frac{3}{2}, 00; \frac{3}{2}\rangle$		0.41	0.20
$\frac{5}{2}^-_2$	$\vert (h_{9/2}^3)\frac{5}{2}, 00; \frac{5}{2}\rangle$	−0.42		
	$\vert (h_{9/2}^3)\frac{9}{2}, 12; \frac{5}{2}\rangle$	−0.55		
	$\Vert (h_{9/2}^2)2, f_{7/2} \vert \frac{5}{2}, 00; \frac{5}{2}\rangle$		0.89	
	$\Vert (h_{9/2}^2)4, f_{7/2} \vert \frac{5}{2}, 00; \frac{5}{2}\rangle$		0.38	
$\frac{1}{2}^-_1$	$\vert (h_{9/2}^3)\frac{5}{2}, 12; \frac{1}{2}\rangle$	0.69		
	$\vert (h_{9/2}^3)\frac{9}{2}, 24; \frac{1}{2}\rangle$	−0.51		
	$\Vert (h_{9/2}^2)4, f_{7/2} \vert \frac{1}{2}, 00; \frac{1}{2}\rangle$	0.32		
	$\Vert (h_{9/2}^2)4, f_{7/2} \vert \frac{1}{2}, 00; \frac{1}{2}\rangle$		0.98	

TABLE I *(Continued)*

		^{205,207,209}At	^{211}At	
		Present	Present	Shell Model [a]
$\frac{3}{2}^-_3$	$\lvert (h_{9/2}{}^3)\frac{7}{2}, 12; \frac{3}{2}\rangle$	−0.54		
	$\lVert (h_{9/2}{}^2)2, f_{7/2} \rvert \frac{3}{2}, 00; \frac{3}{2}\rangle$		−0.41	
	$\lVert (h_{9/2}{}^2)0, f_{7/2} \rvert \frac{7}{2}, 12; \frac{3}{2}\rangle$	0.39		
	$\lvert (h_{9/2}{}^3)\frac{3}{2}, 00; \frac{3}{2}\rangle$	−0.30		
	$\lvert (h_{9/2}{}^3)\frac{3}{2}, 12; \frac{3}{2}\rangle$	−0.32		
	$\lVert (h_{9/2}{}^2)4, f_{7/2} \rvert \frac{3}{2}, 00; \frac{3}{2}\rangle$		0.89	
$\frac{5}{2}^-_3$	$\lvert (h_{9/2}{}^3)\frac{5}{2}, 00; \frac{5}{2}\rangle$	0.30		
	$\lVert (h_{9/2}{}^2)2, f_{7/2} \rvert \frac{5}{2}, 00; \frac{5}{2}\rangle$	−0.56		
	$\lVert (h_{9/2}{}^2)0, f_{7/2} \rvert \frac{7}{2}, 12; \frac{5}{2}\rangle$	−0.46		
	$\lVert (h_{9/2}{}^2)2, f_{7/2} \rvert \frac{5}{2}, 00; \frac{5}{2}\rangle$		0.35	
	$\lVert (h_{9/2}{}^2)4, f_{7/2} \rvert \frac{5}{2}, 00; \frac{5}{2}\rangle$		−0.64	
	$\lVert (h_{9/2}{}^2)6, f_{7/2} \rvert \frac{5}{2}, 00; \frac{5}{2}\rangle$		−0.65	

[a] Reference 16.

of the vibrator charge[24, 25, 28] is expressed by $e^{\mathrm{VIB}} = \frac{4}{3}\pi(1/R_0{}^2)[B^{\mathrm{VIB}}(E2)(2_1^+ \to 0_1^+)]^{1/2}$. The symbol $b_2^{\mu\dagger}$ is the phonon creation operator and $\vec{\mathrm{S}}$ is the spin operator. The electromagnetic operators are obtained by calculating the matrix elements of the $M(E2)$ and $M(M1)$ operators using the wave functions from diagonalization. Tables II and III give the calculated electromagnetic properties corresponding to the wave functions, the main components of which are listed in Table I. In this calculation we chose the value of the vibrator charge $e^{\mathrm{VIB}} = 2$, as used in the calculations for Tl, Hg, and Au.[25] For nuclei away from doubly-closed shells the value of the single-particle charge $e^{\mathrm{s.p.}}$ is 2, and for ^{211}At it is 1.5.[24, 25] For the gyromagnetic ratios we use $g_R = Z/A$, $g_l = 1$, and $g_s = 0.7 g_s^{\mathrm{free}}$.[24, 25, 28]

In the present calculation the basic vibrator was assumed to be harmonic, i.e., the physical anharmonicities related to the quadrupole moment of the one-phonon state and to the splitting of the two-phonon multiplet are neglected. The quadrupole moment of one-phonon states in even Pb isotopes is theoretically predicted to be small.[30] On the other hand, the one-phonon components in low-lying states are not sizeable. The two-phonon components in the wave functions of low-lying states are small and, therefore, their properties are not very sensitive to the two-phonon interaction. The general influence of explicit phonon anharmonicities on the present model is discussed in Refs. 27 and 31.

III. DISCUSSION

The lowest group of negative-parity states in odd At isotopes is based on $(h_{9/2}{}^3)\frac{9}{2}^-$ and

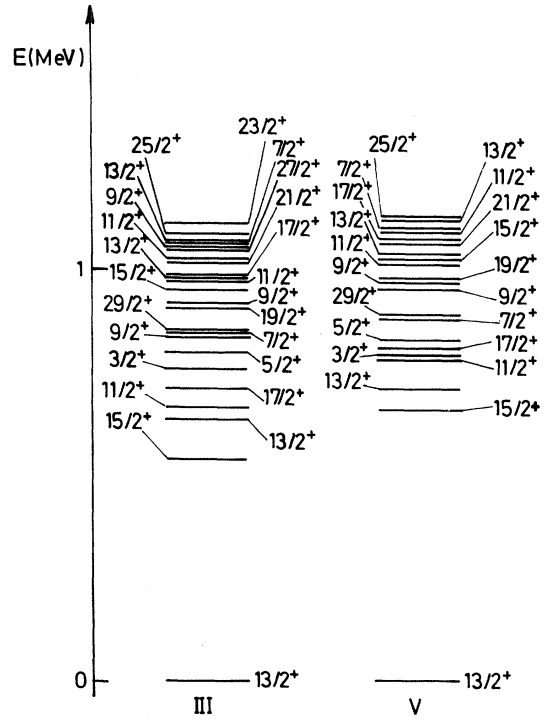

FIG. 2. Calculated positive-parity spectra of odd At isotopes. For description see Sec. II. The origin of the energy scale is placed arbitrarily.

$|(h_{9/2}{}^2)0, f_{7/2}|\frac{7}{2}^-$ states of seniority one and $(h_{9/2}{}^3)\frac{3}{2}^-$, $\frac{5}{2}^-$, $\frac{7}{2}^-$, $\frac{9}{2}^-$, $\frac{11}{2}^-$, $\frac{13}{2}^-$, $\frac{15}{2}^-$, $\frac{17}{2}^-$, $\frac{21}{2}^-$ states of seniority three, as in the case of shell-model calculations for three particles. The mixing of $(h_{9/2}{}^3)\frac{9}{2}^-$ states of seniority one and three is very weak, while the mixing of the two $\frac{7}{2}^-$ basic states $(h_{9/2}{}^3)\frac{7}{2}^-$ and $|(h_{9/2}{}^2)0, f_{7/2}|\frac{7}{2}$ is sizeable. Small one-phonon admixtures relatively slightly affect the wave functions but appreciably increase the electric moments (static and transition) through the coherence mechanism.[27,31] The main components of the wave functions resemble those in shell-model calculations. For these states the present calculation corresponds approximately to the shell-model calculation with the pairing plus quadrupole-quadrupole force and with the effective charge included. In fact, the exchange of a phonon between valence-shell particles involves the same topology as the matrix element of the Q-Q component of the residual interaction. The similarity between our results and those of the shell-model calculation for lowest-lying states in ^{211}At can easily be seen from comparison in Table I. The amplitudes of the dominant components are larger in the shell-model calculation than in our results, since we explicitly included admixtures of phonon multiplets; thus the basic components were additionally renormalized. It should be pointed out that only pairing and quadrupole-quadrupole correlations are included in the present model. However, in the case of ^{211}At with three particles outside of the doubly-closed shell ^{208}Pb nucleus the effective particle-vibration coupling strength $a/\hbar\omega_2$ is small. Therefore, the other components of the residual force also become important, giving mainly diagonal contributions. This leads to shifts in energies, without sizeably affecting other properties. In the present description of ^{211}At the resulting spectrum is, therefore, poorer than the electromagnetic properties.

The effective particle-vibration coupling strength

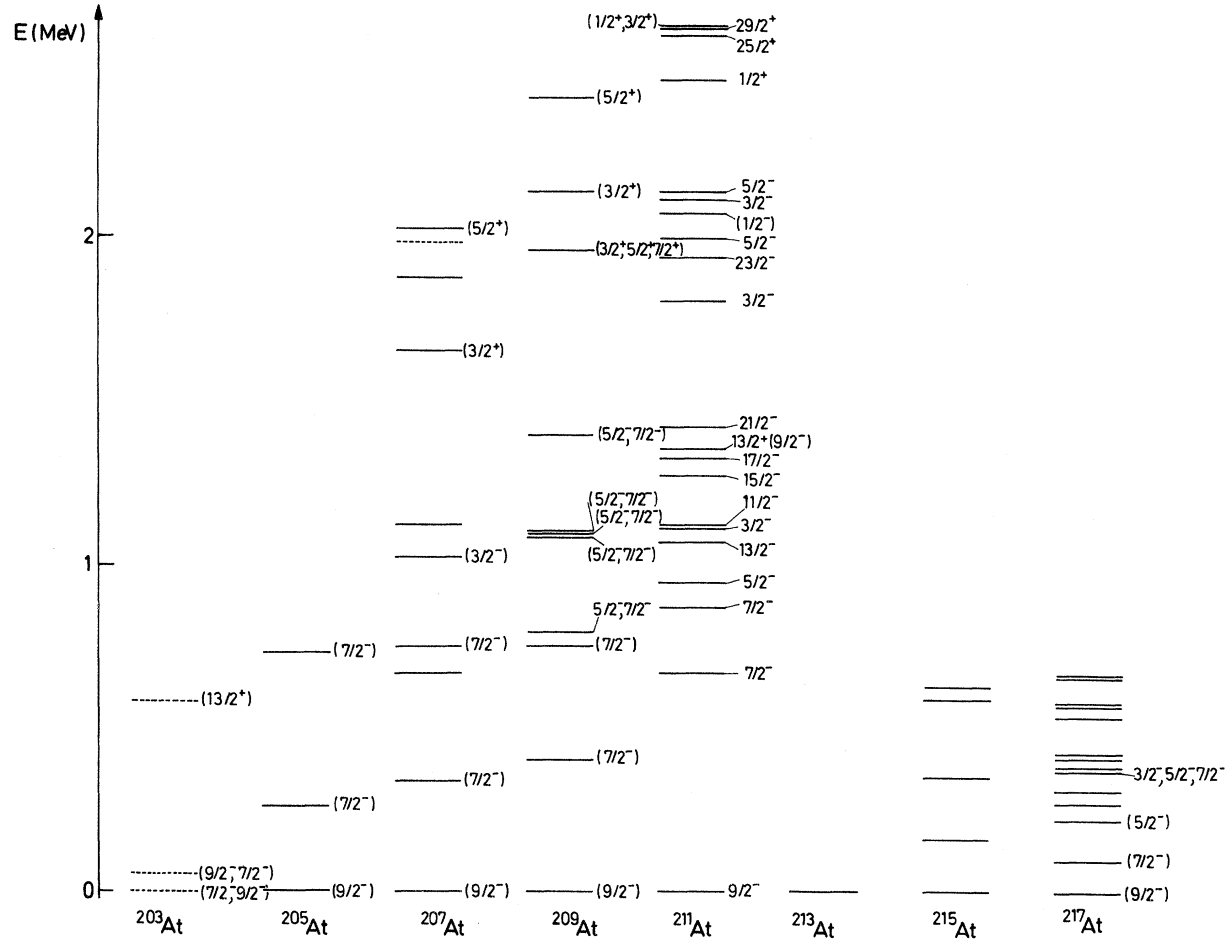

FIG. 3. Available experimental spectra of odd At isotopes (Refs. 1--14).

$a/\hbar\omega_2$ becomes appreciably larger in the region of nuclei away from the doubly-closed shell vibrator, and the role of the particle-vibration interaction in the formation of spectra becomes more important relative to the other components of the residual force.

However, the lowest group of states retains its predominantly particle character, although the admixtures of phonon multiplets increase. The only qualitative change consists in the exchange of character of the two lowest $\frac{7}{2}^-$ states.

In ^{211}At, states which follow the group of low-lying states are based on $|(h_{9/2}{}^2)J\neq 0, f_{7/2}|I$ configurations. The low-spin states of this group are $|(h_{9/2}{}^2)2, f_{7/2}|\frac{3}{2}^-, \frac{5}{2}^-$, $|(h_{9/2}{}^2)4, f_{7/2}|\frac{1}{2}^-, \frac{3}{2}^-, \frac{5}{2}^-$, and $|(h_{9/2}{}^2)6, f_{7/2}|\frac{5}{2}^-$. These states are expected to be populated by the radioactive decay of ^{211}Rn ($\frac{1}{2}^-$). Indeed, in the energy region at about 2 MeV five states, $\frac{3}{2}^-$, $\frac{5}{2}^-$, $(\frac{1}{2}^-)$, $\frac{3}{2}^-$, and $\frac{5}{2}^-$, were observed. These might correspond to the model states. Such shell-model identification was previously suggested in shell-model calculations.[5,20]

In other At isotopes, states which follow the lowest group also involve sizeable components of the one-phonon multiplet $|(h_{9/2}{}^3)\frac{9}{2}, 12; \frac{5}{2}^-, \frac{7}{2}^-, \frac{9}{2}^-, \frac{11}{2}^-, \frac{13}{2}^-\rangle$. The other multiplets, $|(h_{9/2}{}^3)^{v=1}\frac{9}{2}, 2R; I\rangle$, $|(h_{9/2}{}^3)^{v=3}\frac{9}{2}, 12; I\rangle$, and $||(h_{9/2}{}^2)0, f_{7/2}|\frac{7}{2}, 12; I\rangle$, are also involved in the corresponding wave functions with not too small amplitudes.

The electromagnetic properties calculated in Sec. II can be discussed in terms of generalized vibrational intensity and selection rules (GVISR). For the intermediate coupling strength, GVISR is based on partial summation of leading diagrams of the perturbation expansion and on the inco-

TABLE II. Calculated and available experimental $B(E2)$ values for transitions between low-lying negative-parity states in ^{211}At and ^{205,207,209}At. The $\frac{7}{2}_2^- \rightarrow \frac{7}{2}_1^-$ transition with $B(M1)=0.37$ and $B(M1)=0.15$ $(\mu_N)^2$ in ^{211}At and ^{205,207,209}At, respectively, is the only sizeable calculated $M1$ transition among those listed in the table. $M1$ transitions between the predominantly $(h_{9/2}{}^3)$ states are strongly hindered by a hindrance factor of $\gtrsim 10^4$. Quantitative estimates for these small values are not reliable because they involve the interference of small terms and, therefore, the sensitivity to details of parametrization.

	^{211}At $B(E2)$ $(e\,\mathrm{b})^2$		^{205,207,209}At
	Th	Exp	$B(E2)$ $(e\,\mathrm{b})^2$
$\frac{7}{2}_1^- \rightarrow \frac{9}{2}_1^-$	0.029		0.174
$\frac{7}{2}_2^- \rightarrow \frac{9}{2}_1^-$	0.028		0.006
$\frac{5}{2}_1^- \rightarrow \frac{9}{2}_1^-$	0.037		0.149
$\frac{13}{2}_1^- \rightarrow \frac{9}{2}_1^-$	0.034		0.148
$\frac{11}{2}_1^- \rightarrow \frac{9}{2}_1^-$	0.017		0.101
$\frac{7}{2}_2^- \rightarrow \frac{7}{2}_1^-$	0.001		0.001
$\frac{5}{2}_1^- \rightarrow \frac{7}{2}_1^-$	0.003		0.019
$\frac{3}{2}_1^- \rightarrow \frac{7}{2}_1^-$	0.005	$\approx$0.003	0.045
$\frac{11}{2}_1^- \rightarrow \frac{7}{2}_1^-$	0.005		0.033
$\frac{5}{2}_1^- \rightarrow \frac{7}{2}_2^-$	0.005		0.001
$\frac{3}{2}_1^- \rightarrow \frac{7}{2}_2^-$	0.010	0.014	0.004
$\frac{11}{2}_1^- \rightarrow \frac{7}{2}_2^-$	0.009		0.001
$\frac{3}{2}_1^- \rightarrow \frac{5}{2}_1^-$	0.081	0.092	0.214
$\frac{11}{2}_1^- \rightarrow \frac{13}{2}_1^-$	0.034		0.079
$\frac{15}{2}_1^- \rightarrow \frac{13}{2}_1^-$	0.005	0.004	0.023
$\frac{17}{2}_1^- \rightarrow \frac{13}{2}_1^-$	0.037		0.117
$\frac{15}{2}_1^- \rightarrow \frac{11}{2}_1^-$	0.019	0.011	0.070
$\frac{17}{2}_1^- \rightarrow \frac{15}{2}_1^-$	0.011		0.052
$\frac{21}{2}_1^- \rightarrow \frac{17}{2}_1^-$	0.022	0.013	0.083

TABLE III. Static electric quadrupole and magnetic dipole moments for negative-parity states in ^{211}At and ^{205,207,209}At.

	^{211}At		^{205,207,209}At	
	Q $(e\,\mathrm{b})$	μ (μ_N)	Q $(e\,\mathrm{b})$	μ (μ_N)
$\frac{9}{2}_1^-$	−0.26	3.30	−0.51	3.28
$\frac{7}{2}_1^-$	−0.50	4.23	−0.99	2.84
$\frac{7}{2}_2^-$	−0.54	3.29	−1.04	4.49
$\frac{5}{2}_1^-$	0.01	1.84	−0.07	2.29
$\frac{13}{2}_1^-$	−0.11	4.77	0.002	0.03
$\frac{3}{2}_1^-$	0.11	1.10	0.18	1.13
$\frac{11}{2}_1^-$	−0.03	4.04	−0.10	3.94
$\frac{15}{2}_1^-$	0.03	5.50	0.04	5.45
$\frac{17}{2}_1^-$	−0.25	6.24	−0.47	6.19
$\frac{21}{2}_1^-$	−0.54	7.71	−1.08	7.70

herence among the remaining higher-order terms.[24, 27, 31]

Here we discuss $E2$ transitions between the cluster states $|J_1\rangle \rightarrow |J_2\rangle$ (i.e., $\Delta N=0$, $N=0$). In zeroth order the transition moment $\langle J_2 \| e^{\text{s.p.}} r^2 Y_2 \| J_1\rangle \equiv e^{\text{s.p.}} \times$(M.E.) is of the single-particle order of magnitude. However, first-order induced collective contributions, which involve the emission or absorption of a virtual phonon and its interaction with the electromagnetic field, can be incorporated into the single-particle charge renormalization, as illustrated diagrammatically[24, 32, 33] in Fig. 4(a). The corresponding renormalized effective charge is $e^1_{\text{eff}}=e^{\text{s.p.}}+(5/2(\pi)^{1/2})e^{\text{VIB}}\ |a|[1/(\hbar\omega_2+E_2-E_1)+1/(\hbar\omega_2-E_2+E_1)]$, where E_2 and E_1 are the energies of the cluster in the initial and final state, respectively, and $|a|$ is the absolute value of the coupling strength a. In the case $E_1=E_2$ this expression becomes $e^1_{\text{eff}}(E_1=E_2)=e^{\text{s.p.}}+[5/(\pi)^{1/2} \times(e^{\text{VIB}}\ |a|/\hbar\omega_2)]$, i.e., it is independent of the cluster state. The effective charge $e^1_{\text{eff}}(E_1=E_2)$ in the case $|J_2\rangle = |J_1\rangle$ corresponds to the static quadrupole moment of the $|J_1\rangle$ state.

There are two types of higher-order contributions to $E2$ moments between cluster states:
(a) Vertex corrections (VC), where the electromagnetic field interacts with the cluster state in the presence of virtual phonons, or with virtual phonons which are created or annihilated by the cluster in the presence of virtual phonons.
(b) Self-energy corrections (SE), which contain the initial- and/or final-state cluster as an intermediate state.

Lowest-order VC and SE are illustrated in Figs. 4(b) and 4(c), respectively. If one takes into account only one cluster configuration and the classical limit of large j (i.e., small angular-momentum transfer), then VC + SE = 0.[27] This is the analog of the Ward identity[34] from field theory; the cluster-vibration $E2$ moment is then exactly equal to the shell-model cluster quadrupole moment with the effective charge e^1_{eff} $(E_1=E_2)$. For $0<|E_1-E_2|<\hbar\omega$ the approximate relation reads[27]

$$(\text{M.E.}+\text{VC}+\text{SE})\,e^1_{\text{eff}} \approx (\text{M.E.})\,e^1_{\text{eff}}(E_1=E_2),$$

i.e., $e^1_{\text{eff}}(E_1=E_2)$ plays the role of the usual shell-model effective charge. Therefore, the corresponding transitions are sizeably enhanced over the single-particle magnitude if (M.E.) does not involve spin-flip. Consequently, non-spin-flip transitions between clusters (i.e., $\Delta N=0$, $N=0$) with $|E_1-E_2|<\hbar\omega$ are in GVISR classified as allowed.

For the parametrizations from Sec. II we have $e^1_{\text{eff}}(E_1=E_2)\approx 2$ for ^{211}At and $e^1_{\text{eff}}(E_1=E_2)\approx 4$ for $^{205, 207, 209}$At. Most transitions between the lowest group of states in odd At isotopes are non-spin-flip, of the type $\Delta N=0$, $N=0$, $|E_1-E_2|<\hbar\omega$, and the calculated $B(E2)$ values from Table II reflect the GVISR prediction.

In the zeroth-order approximation the two lowest $\frac{7}{2}^-$ states are $|\frac{7}{2}_1^{(0)}\rangle \equiv \|(h_{9/2}{}^2)0, f_{7/2}|\frac{7}{2}\rangle$ and $|\frac{7}{2}_2^{(0)}\rangle \equiv |(h_{9/2})^3\frac{7}{2}\rangle$, respectively. By including the particle-field coupling the $|\frac{7}{2}_2^{(0)}\rangle$ state is strongly pushed down with respect to the other states due to one-phonon admixtures, and this state may even become the ground state if the coupling strength is sufficiently strong ("$I=j-1$ anomaly").[24] Such a situation might appear in neutron-deficient At isotopes $A \lesssim 203$.[10] The scarce experimental information indicates that the $\frac{7}{2}_1^-$ state might be the ground state of ^{203}At, and/or the $\frac{7}{2}_1^-$ and $\frac{9}{2}_1^-$ states lie very close.[9, 10] The lowering of the $\frac{7}{2}_1^-$ state can also be understood in the deformed representation, where the $\frac{7}{2}^-|514|$ state becomes the ground state.[9] It should be stressed that generally, both the spherical representation (coupling of the spherical shell-model cluster to vibrations) and the deformed representation (coupling of Nilsson states to rotations) can be successfully used in describing the properties of nuclei lying close

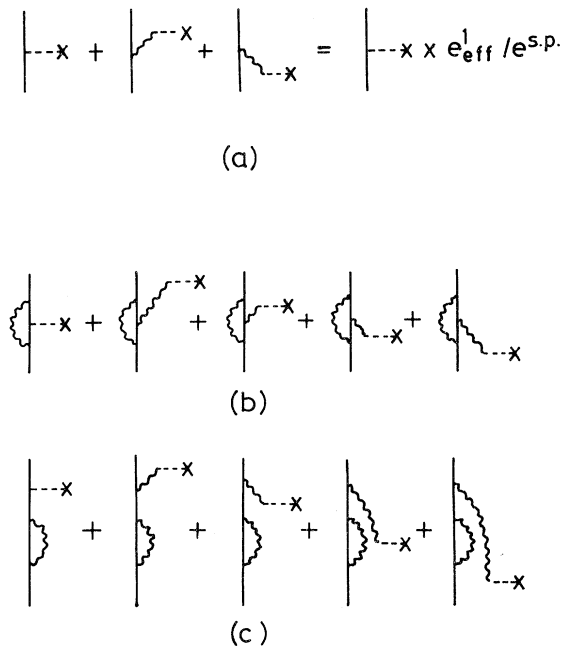

FIG. 4. Leading diagrams for $E2$ moments between cluster states. (a) Zeroth-order diagram and first-order induced collective diagrams contributing to the $E2$ moment. The solid lines correspond to cluster states; the wavy lines are phonons, and the dotted lines with × at the free end represent the interaction with the electromagnetic field. (b) Lowest-order vertex corrections to the $E2$ moment between cluster states. (c) Lowest-order self-energy corrections to the $E2$ moment between cluster states.

to the transitional region.[24] This situation is analogous to that, for example, for the $(g_{9/2}^3)\frac{7}{2}$ configuration in odd Ag isotopes.[24] In $\cdots{}^{203,\,205,\,207,\,209,\,213,\,215,\,217,}\cdots$At isotopes we therefore expect the lowering of the dressed $|\frac{7}{2}_2^{(0)}\rangle$ state. Thus for the intermediate values of the effective coupling strength we expect the first $\frac{7}{2}^-$ state to be based on the $|\frac{7}{2}^{(0)}\rangle$ component. Since in ^{211}At the effective particle-vibration coupling strength $a/\hbar\omega$ is considerably smaller, the $\frac{7}{2}_1^-$ and $\frac{7}{2}_2^-$ states retain their zeroth-order character. The basic component of the $\frac{7}{2}_1^-$ and $\frac{7}{2}_2^-$ states is reflected in the $\frac{7}{2}_1^- \to \frac{9}{2}_1^-$ and $\frac{7}{2}_2^- \to \frac{9}{2}_1^-$ $M1$ transitions. The $\frac{7}{2}_1^{(0)} \to \frac{9}{2}_1^-$ transition is l forbidden and, therefore, small in the framework of the present model. However, velocity-dependent interactions may give additional contributions of the order of magnitude of $0.1\mu_N$ to the corresponding transition moments.[28] On the other hand, the $\frac{7}{2}_2^{(0)} \to \frac{9}{2}_1^-$ transition is of the type $(j^3)J \to (j^3)J' \neq J$ and, therefore, exactly forbidden.[35] This shell-model feature is conserved in the present calculation owing to the smallness and incoherence of higher-order contributions. The corresponding $B(M1)$ values are of the order of magnitude of $\lesssim 10^{-4}(\mu_N)^2$, the magnitude itself being sensitive to parametrization and truncation. The $\frac{7}{2}_1^- \to \frac{9}{2}_1^-$ and $\frac{7}{2}_2^- \to \frac{9}{2}_1^-$ $M1$ transitions in ^{211}At are, therefore, expected to be moderately and strongly hindered, respectively, while in other odd At isotopes the situation is reversed. The $\frac{7}{2}_1^- \to \frac{9}{2}_1^-$ $M1$ transitions in the latter nuclei are predicted to be more hindered than the $\frac{7}{2}_2^- \to \frac{9}{2}_1^-$ transitions.

In ^{211}At the $\frac{7}{2}_1^- \to \frac{9}{2}_1^-$ $E2$ transition is spin-flip forbidden in zeroth order. On the other hand, this transition is increased due to the particle-vibrator coupling; this is, in fact, a $(\Delta N = 0, N = 0)$ transition between the states on the yrast line.[27, 31] The $\frac{7}{2}_2^- \to \frac{9}{2}_1^-$ transition is not forbidden but involves a state away from the yrast line. Therefore, the $\frac{7}{2}_1^- \to \frac{9}{2}_1^-$ and $\frac{7}{2}_2^- \to \frac{9}{2}_1^-$ $E2$ transitions in ^{211}At are predicted in GVISR to be moderately enhanced over the single-particle magnitude. In ^{205,207,209}At the $\frac{7}{2}_1^- \to \frac{9}{2}_1^-$ $E2$ transition is allowed (yrast states, and no selection rule is violated) and the $\frac{7}{2}_2^- \to \frac{9}{2}_1^-$ $E2$ transition is forbidden. These predictions are in agreement with the available experimental data for ^{211}At ($\frac{7}{2}_1^- \to \frac{9}{2}_1^-$ is of the $M1 + E2$ type and $\frac{7}{2}_2^- \to \frac{9}{2}_1^-$ is of the $E2$ type)[5] and ^{207,209}At ($\frac{7}{2}_1^- \to \frac{9}{2}_1^-$ is of the $E2$ type and $\frac{7}{2}_2^- \to \frac{9}{2}_1^-$ is of the $M1$ type).[10]

The exchange of character of the $\frac{7}{2}_1^-$ and $\frac{7}{2}_2^-$ states in lighter At isotopes is also reflected in the population of these states in the radioactive decay of Rn. In the ^{209}Rn ($\frac{5}{2}^-$) decay the $\frac{7}{2}_1^-$ and $\frac{7}{2}_2^-$ states in ^{209}At are populated by logft values of 6.7 and 6.1, respectively.[13, 10] This indicates that the amplitude of the $|(h_{9/2}^2)0, f_{7/2}|\frac{7}{2}$ component in the $\frac{7}{2}_2^-$ state is larger than that of such a component in the $\frac{7}{2}_1^-$ state. An analogous situation appears for the $\frac{7}{2}_1^-$ and $\frac{7}{2}_2^-$ states in ^{205,207}At isotopes.[10] For other low-lying states in ^{209}At below 1.9 MeV the logft value is >7.[13] This indicates that the low-lying $\frac{5}{2}^-$ states contain small admixtures of the $|(h_{9/2}^2)0, f_{5/2}|\frac{5}{2}$ component. In our calculation the corresponding amplitudes amount to 2%, 2%, and 1% for the $\frac{5}{2}_1^-$, $\frac{5}{2}_2^-$, and $\frac{5}{2}_3^-$ states, respectively.

In ^{211}At the $\frac{7}{2}_2^- \to \frac{7}{2}_1^-$ transition is forbidden in zeroth order, so we consider the contributions coming from the mixing of $\frac{7}{2}_1^{(0)}$ and $\frac{7}{2}_2^{(0)}$ states, i.e., from the components

$$|\tfrac{7}{2}_1^-\rangle = -|c\,\|\,\tfrac{7}{2}_1^{(0)}\rangle + |c'\,\|\,\tfrac{7}{2}_2^{(0)}\rangle\,,$$

$$|\tfrac{7}{2}_2^-\rangle = |d\,\|\,\tfrac{7}{2}_1^{(0)}\rangle + |d'\,\|\,\tfrac{7}{2}_2^{(0)}\rangle\,,$$

where $|cd| \approx |c'd'|$.

The $\frac{7}{2}_2^- \to \frac{7}{2}_1^-$ $E2$ and $M1$ transitions are then dominated by

$$\langle \tfrac{7}{2}_1^- \| M(E2) \| \tfrac{7}{2}_2^- \rangle = \left(-|cd| \langle \tfrac{7}{2}_1^{(0)} \left| \sum_{i=1}^{3} Y_2(i) \right| \tfrac{7}{2}_1^{(0)} \rangle + |c'd'| \langle \tfrac{7}{2}_2^{(0)} \left| \sum_{i=1}^{3} Y_2(i) \right| \tfrac{7}{2}_2^{(0)} \rangle \right) \langle r^2 \rangle e^1_{\text{eff}}\,,$$

and

$$\langle \tfrac{7}{2}_1^- \| g_s \vec{S} \| \tfrac{7}{2}_2^- \rangle = (-|cd| \langle \tfrac{7}{2}_1^{(0)} \| \vec{S} \| \tfrac{7}{2}_1^{(0)} \rangle + |c'd'| \langle \tfrac{7}{2}_2^{(0)} \| \vec{S} \| \tfrac{7}{2}_2^{(0)} \rangle) g_s\,,$$

respectively. Since the non-spin-flip matrix elements are of the same order of magnitude and since the terms of this type also appear in the induced collective terms (GVISR), the selection rules for the $\frac{7}{2}_2^- \to \frac{7}{2}_1^-$ $E2$ and $M1$ transitions are essentially given by the relative signs of the reduced matrix elements

$$\langle \tfrac{7}{2}_2^{(0)} \left| \sum_{i=1}^{3} Y_2(i) \right| \tfrac{7}{2}_2^{(0)} \rangle \sim \langle h_{9/2} \| Y_2 \| h_{9/2} \rangle < 0\,,$$

$$\langle \tfrac{7}{2}_1^{(0)} \left| \sum_{i=1}^{3} Y_2(i) \right| \tfrac{7}{2}_1^{(0)} \rangle \sim \langle f_{7/2} \| Y_2 \| f_{7/2} \rangle < 0\,,$$

$$\langle \tfrac{7}{2}_2^{(0)} \| \vec{S} \| \tfrac{7}{2}_2^{(0)} \rangle \sim \langle h_{9/2} \| \vec{S} \| h_{9/2} \rangle < 0\,,$$

and

$$\langle \tfrac{7}{2}_1^{(0)} \| \vec{S} \| \tfrac{7}{2}_1^{(0)} \rangle \sim \langle f_{7/2} \| \vec{S} \| f_{7/2} \rangle \quad > 0 .$$

Therefore, the $\frac{7}{2}^-_2 \to \frac{7}{2}^-_1$ $E2$ transition involves incoherence and is hindered, while the $M1$ transition involves coherence between the main terms. In the degenerate case and classical limit of large angular momenta such a selection rule becomes exact. Thus the $\frac{7}{2}^-_2 \to \frac{7}{2}^-_1$ transition is predicted to be predominantly of the $M1$ type. This is reflected both in the results of calculation in Table II and in experiment. Since in At isotopes away from the neutron closed shell the effective particle-vibration coupling strength is larger, the wave functions are more complex and the $\frac{7}{2}^-_1$ and $\frac{7}{2}^-_2$ states exchange their basic character, but the particle-vibration coupling mechanism preserves the same qualitative features.

$M1$ transitions between the states which are based on $(h_{9/2}{}^3)I$ configurations are forbidden in zeroth order.[35] This shell-model feature is conserved in the coupled system because of the repetition of the same shell-model clusters and due to the incoherence between partial contributions. Thus the absence of strong $M1$ transitions is a characteristic feature of the low-lying part of the spectrum. $M1$ transitions between the $\|(h_{9/2}{}^2)0, f_{7/2}|\frac{7}{2}\rangle$ and $|(h_{9/2}{}^3)J\rangle$ states are l forbidden, but additional velocity-dependent forces relax the retardation.

$E2$ transitions between the yrast states are generally strongly enhanced due to GVISR, except if they are additionally hindered because of the change of the basic cluster (spin-flip or vanishing matrix element).[31] The $B(E2)$ values for transitions between states based on the $(h_{9/2}{}^3)J$ and $(h_{9/2}{}^3)J'$ configurations are in GVISR proportional to $1/(2J+1)|\langle J' \| Y_2 \| J \rangle|^2$.

Since the reduced matrix elements for $J = \frac{3}{2} \to J' = \frac{5}{2}$ are of similar magnitude, as most of the other large matrix elements between $(h_{9/2}{}^3)$ configurations, and since the corresponding statistical factor involves the smallest angular momentum, this $E2$ transition is predicted to be the strongest one.

$\Delta N = 1$ transitions from higher-lying one-phonon multiplet states to $(h_{9/2}{}^3)$ cluster states are hindered in GVISR.[24, 27, 31]

$\frac{3}{2}^-_1 \to \frac{7}{2}^-_1$ and $\frac{3}{2}^-_1 \to \frac{7}{2}^-_2$ $E2$ transitions also reflect the structure of the $\frac{7}{2}^-_1$ and $\frac{7}{2}^-_2$ states. Since $\frac{3}{2}^-_1 \to \frac{7}{2}^0_1$ and $\frac{3}{2}^-_1 \to \frac{7}{2}^0_2$ $E2$ transitions involve vanishing and non-spin-flip matrix elements, respectively, the $B(E2)(\frac{3}{2}^-_1 \to \frac{7}{2}^-_1)/B(E2)(\frac{3}{2}^-_1 \to \frac{7}{2}^-_2)$ ratio is approximately equal to the ratio of squares of amplitudes for the $|\frac{7}{2}^0_2\rangle$ component in the corresponding wave functions. In ^{211}At the value of the experimental ratio $(0.003/0.014) \approx 0.2$ should be compared with the ratio of squares of amplitudes $[(0.53)^2/(0.81)^2] \approx 0.4$. Thus, there is indirect evidence that the $\frac{7}{2}^0_2$ strength is split with more strength being contained in the $\frac{7}{2}^-_2$ state. Quantitatively, the mixing between the $\frac{7}{2}^-_1$ and $\frac{7}{2}^-_2$ states seems to be somewhat overestimated in our parametrization used for ^{211}At. For $^{205, 207, 209}$At the theoretical prediction is opposite, i.e., $B(E2)(\frac{3}{2}^-_1 \to \frac{7}{2}^-_1)/B(E2)(\frac{3}{2}^-_1 \to \frac{7}{2}^-_2) = [(0.66)^2/(0.24)^2] \approx 8$. No experimental information on this ratio is available.

Thus, our conclusions on the structure of the $\frac{7}{2}^-_1$ and $\frac{7}{2}^-_2$ states in $^{205, 207, 209}$At drawn from $B(M1)(\frac{7}{2}^-_1 \to \frac{9}{2}^-_1)$, $B(M1)(\frac{7}{2}^-_2 \to \frac{9}{2}^-_1)$, and $B(E2)(\frac{3}{2}^-_1 \to \frac{7}{2}^-_1)$, $B(E2)(\frac{3}{2}^-_1 \to \frac{7}{2}^-_2)$, and ft values in the radioactive decay of $^{205, 207, 209}$Rn, respectively, are mutually consistent.

The mechanism of the particle-field coupling creates two sequences of strong $\Delta I = 2$ $E2$ transitions along the yrast line, which resemble the "decoupled" bands in odd deformed nuclei. This is a general feature of the present model.[24, 27] This quasirotational feature is partly dissolved in the low-lying part of the spectrum. The experimental $\frac{21}{2}^-_1 \to \frac{17}{2}^-_1 \to \frac{13}{2}^-_1 \to \frac{9}{2}^-_1$ $E2$ cascade[11] represents an element of the $\Delta I = 2$ sequence on the yrast line.

The lowest-lying positive-parity state $\frac{13}{2}^+_1$ is based on the $\|(h_{9/2}{}^2)0, i_{13/2}|\frac{13}{2}, 00; \frac{13}{2}^+\rangle$ configuration, which amounts to 97% in the ^{211}At and 56% in the $^{205, 207, 209}$At wave function. The following group of positive-parity states is largely based on the $\|(h_{9/2}{}^2)J \neq 0, i_{13/2}|I, 00; I^+\rangle$ configurations. Because of several available degenerate basis states of the same spin (differing only in the intermediate angular momentum J) the positive-parity states in that region are rather dense. As an example, we present the main components in the wave functions of two lowest $\frac{15}{2}^+$ states in ^{211}At:

$$\begin{aligned} |\tfrac{15}{2}^+_1\rangle &= 0.83\,\|(h_{9/2}{}^2)2, i_{13/2}|\tfrac{15}{2}\rangle \\ &\quad + 0.49\,\|(h_{9/2}{}^2)4, i_{13/2}|\tfrac{15}{2}\rangle , \\ |\tfrac{15}{2}^+_2\rangle &= 0.46\,\|(h_{9/2}{}^2)2, i_{13/2}|\tfrac{15}{2}\rangle \\ &\quad - 0.62\,\|(h_{9/2}{}^2)4, i_{13/2}|\tfrac{15}{2}\rangle \\ &\quad - 0.54\,\|(h_{9/2}{}^2)6, i_{13/2}|\tfrac{15}{2}\rangle . \end{aligned}$$

In $^{205, 207, 209}$At the strength is more split, and one-phonon admixtures become sizeable.

At about 2.6 MeV one expects the octupole-phonon septuplet $|(h_{9/2}{}^3)^{(v=1)}\frac{9}{2}, 13^-; I = \frac{3}{2}^+, \ldots, \frac{15}{2}^+\rangle$ to be analogous to the well-known septuplet in ^{209}Bi.[32, 33, 36-38] The admixtures of these states to the negative-parity states of the present model are small, because the matrix element

$$\langle\, |(h_{9/2}{}^2)J, i_{13/2}|I|\, \Big|\sum_{i=1}^{3} Y_3(i)\Big|\, |(h_{9/2}{}^3)\tfrac{9}{2}\rangle$$

is of the spin-flip type and, therefore, small. The pairing-phonon multiplets expected in the same energy region are $|s_{1/2}{}^{-1}, 10_p^+; \frac{1}{2}^+\rangle$, $|d_{3/2}{}^{-1}, 10_p^+; \frac{3}{2}^+\rangle$, $|d_{5/2}{}^{-1}, 10_p^+; \frac{5}{2}^+\rangle$, $|s_{1/2}{}^{-1}, 12_p^+; I=\frac{3}{2}^+, \frac{5}{2}^+\rangle$, $|d_{3/2}{}^{-1}, 12_p^+; I=\frac{1}{2}^+, \frac{3}{2}^+, \frac{5}{2}^+, \frac{7}{2}^+\rangle$ etc. The pairing phonons 0_p^+, 2_p^+ are the correlated states in the particle-particle channel and correspond to the states from the neighboring even Rn isotopes. The first two pairing-phonon multiplet states are appreciably populated in ^{211}At by the decay of ^{211}Rn,[5] while the second and third pairing-phonon multiplet states are populated in lighter At isotopes by radioactive decay.[13] This situation is similar to that in ^{209}Bi, where pairing phonons are states from ^{210}Po. The coupling between octupole and pairing-phonon multiplets may be sizeable[36-38] but pairing phonons are weakly coupled to our positive-parity model states, because in leading order they differ microscopically in at least two single-particle configurations $(s_{1/2}{}^{-1}h_{9/2}{}^4 - h_{9/2}{}^2 i_{13/2})$.

IV. CONCLUSION

In the present work the interplay of three valence-shell protons outside of the $Z=82$ closed shell and the low-frequency vibrational field is presented for the case of odd At isotopes. This mechanism accounts for the explicit appearance of broken and promoted pairs, as well as for part of the anharmonic structure created by the cluster-phonon interaction (i.e., anharmonicities from the neighboring even Po isotopes). The present approach provides a simple understanding of the main experimental properties of odd At isotopes. However, the quantitative results should not be interpreted too rigidly because of the neglected modes and correlations. Especially the relative importance of the particle-vibration coupling for ^{211}At is diminished because of the substantially smaller effective coupling strength.

The author expresses his gratitude to Professor G. Alaga for valuable discussions.

---

*Part of this work was performed during the author's stay at the International Centre for Theoretical Physics, Trieste, Italy.

[1]I. Bergström, B. Fant, C. J. Herrlander, P. Thieberger, K. Wikström, and G. Astner, Phys. Lett. 32B, 476 (1970).
[2]I. Bergström, B. Fant, C. J. Herrlander, K. Wikström, and J. Blomqvist, Physica Scripta 1, 243 (1970).
[3]K. H. Maier, J. R. Leigh, F. Pühlhofer, and R. M. Diamond, Phys. Lett. 35B, 401 (1971).
[4]A. W. Stoner, UCRL Report No. UCRL-3471, 1956 (unpublished); C. M. Lederer, J. M. Hollander, and I. Perlman, *Table of Isotopes* (Wiley, New York, 1967); H. L. Garvin, T. M. Green, E. Lipworth, and W. A. Nierenberg, Phys. Rev. Lett. 1, 74 (1958).
[5]G. Astner, Physica Scripta 5, 31 (1972).
[6]G. Astner and V. Berg, Physica Scripta 5, 55 (1972).
[7]G. Astner, I. Bergström, J. Blomqvist, B. Fant, and K. Wikström, Nucl. Phys. A182, 219 (1972).
[8]T. Kempisti, T. Morek, L. K. Peker, K. Petrozolin, and S. Hoinacki, JINR, Dubna, Report No. P6-5878, 1971.
[9]T. Morek, V. Noibert, S. Hoinacki, K. Aleksander, and Z. Vil'gel'mi, JINR, Dubna, Report No. P6-4494, 1969.
[10]T. Kempist'i, A. Korman, T. Morek, L. K. Peker, Nguen Tat To, E. Haratim, and S. Hoinacki, JINR, Dubna, Report No. P6-7003, 1973.
[11]B. S. Dzhelepov, R. B. Ivanov, M. A. Mihajlova, and V. O. Sergeev, Izv. Akad. Nauk SSSR Ser. Fiz. 36, 2080 (1972).
[12]Tz. V'ilov, N. A. Golovkov, K. Ya. Gromov, I. I. Gromova, A. Kolachkovski, M. Ya. Kuznetsova, Yu. V. Norseev, and V. G. Chumin, Izv. Akad. Nauk SSSR Ser. Fiz. 38, 701 (1974).
[13]Tz. V'ilov, N. A. Golovkov, I. I. Gromova, A. Kolachkovski, M. Ya. Kuznetzova, Yu. V. Norseev, and V. G. Chumin, JINR, Dubna, Report No. P6-6767, 1972.
[14]Nucl. Data B1(No. 5), 1 (1966); *ibid.* B10(No. 6), 611 (1973).
[15]R. Arvieu, O. Bohigas, and C. Quesne, Nucl. Phys. A143, 577 (1970).
[16]V. I. Isakov, T. A. Kozhamkulov, and L. A. Sliv, Izv. Akad. Nauk SSSR, Ser. Fiz. 36, 798 (1972).
[17]Yu. I. Haritonov, L. K. Peker, and L. A. Sliv, Fiziko-Technicheski Institut Report No. 307, 1970.
[18]L. A. Sliv, *Tezisny doklad XXI Ezhegodnogo Soveschania po yadernoy spektroskopii i strukture atomnogo yadra* (Nauka, Moskva, 1971).
[19]N. Freed and J. Gibbons, as quoted in Ref. 5.
[20]J. Blomqvist, Research Institute for Physics, 1970, Annual Report, contribution No. 3.8.2 (unpublished).
[21]J. Blomqvist, J. Phys. Soc. Jpn. 34, 223 (1973).
[22]G. M. Ewart, W. J. Gerace, and J. F. Walker, Nucl. Phys. A191, 596 (1972).
[23]G. Alaga, Bull. Am. Phys. Soc. 4, 359 (1959).
[24]V. Paar, Nucl. Phys. A211, 29 (1973); Phys. Lett. 39B, 466 (1972); 39B, 587 (1972); 42B, 8 (1972); Z. Phys. 271, 11 (1974); and to be published.
[25]G. Alaga and G. Ialongo, Nucl. Phys. A97, 600 (1967); G. Alaga, *Rendiconti Scuola Internazionale ti Fisica "E. Fermi", Varenna, XL Corso* (Academic, New York, 1967), p. 28.
[26]R. Almar, O. Civitarese, F. Krmpotić, and J. Navaza, Phys. Rev. C 6, 187 (1972).
[27]G. Alaga and V. Paar, unpublished.
[28]A. Bohr and B. R. Mottelson, K. Dan. Vidensk. Selsk. Mat.—Fys. Medd. 27, No. 16 (1953).
[29]R. A. Broglia, V. Paar, and D. R. Bes, Phys. Lett. 37B, 257 (1971).

[30]R. A. Broglia, R. Liotta, and V. Paar, Phys. Lett. 38B, 480 (1972).
[31]G. Alaga, F. Krmpotić, V. Lopac, V. Paar, and L. Šips, unpublished; V. Paar, Proceedings of Extended Seminar on Nuclear Physics, Trieste 1974 (IAEA, Vienna, to be published).
[32]A. Bohr and B. R. Mottelson, Annu. Rev. Nucl. Sci. 23, 363 (1973).
[33]I. Hamamoto, Nucl. Phys. A126, 545 (1969); A135, 576 (1969).
[34]S. S. Schweber, *An Introduction to Relativistic Quantum Field Theory* (Row, Peterson, and Co., New York, 1961).
[35]A. de-Shalit and I. Talmi, *Nuclear Shell Theory* (Academic, New York, 1963).
[36]J. W. Hertel, D. G. Fleming, J. P. Schiffer, and H. E. Gove, Phys. Rev. Lett. 23, 488 (1969).
[37]R. A. Broglia, R. Liotta, and V. Paar, unpublished.
[38]D. Zawischa, Z. Phys. 266, 117 (1974).